



RESEARCH LETTER

10.1029/2018GL078558

Key Points:

- Internal multidecadal variability is an important modulator of the tropical climate response to CO₂ forcing
- By impacting global atmospheric energetics, AMOC fluctuations affect the strength of the mean atmospheric tropical circulation
- The dependence of the CO₂-forced circulation response to AMOC-related background state follows a *strong-gets-weaker* pattern

Supporting Information:

- Supporting Information S1
- Figure S1
- Figure S2
- Figure S3
- Figure S4
- Figure S5
- Figure S6
- Figure S7
- Figure S8
- Figure S9
- Figure S10
- Figure S11
- Figure S12
- Figure S13
- Figure S14

Correspondence to:

J. Vial,
jessica.vial@mpimet.mpg.de

Citation:

Vial, J., Cassou, C., Codron, F., Bony, S., & Ruprich-Robert, Y. (2018). Influence of the Atlantic Meridional Overturning Circulation on the tropical climate response to CO₂ forcing. *Geophysical Research Letters*, 45, 8519–8528. <https://doi.org/10.1029/2018GL078558>




Received 30 APR 2018

Accepted 4 AUG 2018

Accepted article online 13 AUG 2018

Published online 24 AUG 2018

Influence of the Atlantic Meridional Overturning Circulation on the Tropical Climate Response to CO₂ Forcing

Jessica Vial^{1,2} , Christophe Cassou³, Francis Codron¹ , Sandrine Bony⁴ , and Yohan Ruprich-Robert⁵

¹LOCEAN/IPSL, Sorbonne Université, CNRS, Université Pierre et Marie Curie, Paris, France, ²Max Planck Institute for Meteorology, Hamburg, Germany, ³Université de Toulouse, CECI, CNRS-Cerfacs, Toulouse, France, ⁴LMD/IPSL, Sorbonne Université, CNRS, Université Pierre et Marie Curie, Paris, France, ⁵Barcelona Supercomputing Center, Barcelona, Spain

Abstract The increase of atmospheric greenhouse gases is expected to affect the hydrological cycle and large-scale precipitation patterns. In parallel, unforced natural variability on decadal-to-multidecadal timescales can also modulate forced changes at the regional scales. Based on multimember ensembles from a coupled General Circulation Model, we investigate the sensitivity of CO₂-forced changes in tropical precipitation and atmospheric circulation to fluctuations of the Atlantic Multidecadal Overturning Circulation (AMOC). We show that contrasted AMOC states yield considerable differences in equatorial Pacific precipitation forced changes, by impacting the direct (within a year) CO₂-induced weakening of the Walker circulation. We use global atmospheric energetics, as a theoretical backdrop, to explain the relationship between the tropical atmospheric circulation and the AMOC state. A physical mechanism is then proposed, relating the direct CO₂-forced weakening of the atmospheric tropical circulation to its climatological strength in unperturbed climate and indirectly to the AMOC state.

Plain Language Summary The precipitation response to increased greenhouse gases atmospheric concentration is one of the most critical factors of the overall impact of climate change. The presence of natural climate variability on decadal-to-multidecadal timescales is expected to modulate the long-term projections at the regional scales. This can be viewed as an irreducible source of uncertainties for the climate response to GHG forcing, which should be quantified and better understood. Based on an ensemble of experiments from a fully coupled General Circulation Model, we quantify and investigate the sensitivity of the CO₂-forced climate response in terms of tropical precipitation and circulation, to the internal fluctuation of the Atlantic Multidecadal Overturning Circulation (AMOC). We show that contrasted states of AMOC, used as initial conditions in increased-CO₂ experiments, yield considerable differences in the tropical precipitation forced changes over Indonesia, Southeast Asia, and the equatorial Pacific Ocean. We provide evidence that the AMOC-related influence on precipitation changes is essentially due to the fast and direct (within a year) CO₂-induced weakening of the Walker circulation. Our findings are further supported by physical understanding based on large-scale atmospheric energetics.

1. Introduction

Predicting the precipitation response to increasing greenhouse gases (GHG) atmospheric concentration remains a great scientific challenge. The need to better anticipate future precipitation changes is particularly strong in the tropics where nearly 50% of the Earth's population is influenced by rainfall and monsoon variability (De Carvalho, 2016). Past investigations have led to considerable progress in our understanding of the key factors controlling the long-term (centuries ahead) precipitation forced response assessed from coupled models under specific GHG emission scenarios (Bony et al., 2013; Chadwick et al., 2013; Chou & Neelin, 2004; Chou et al., 2009; Held & Soden, 2006; Seager et al., 2010; Xie et al., 2010). Physical mechanisms have also been proposed to explain the considerable spread among the models' projections (Long et al., 2016; Ma & Xie, 2013; Oueslati et al., 2016; Xie et al., 2015). On the other hand, few studies so far have evaluated the importance of the decadal-to-multidecadal internal variability in modulating the long-term response of regional rainfall to anthropogenic forcing (Cassou et al., 2018; Xie et al., 2015), despite the dominant contribution of natural climate variability to uncertainties in regional precipitation projections (Hawkins & Sutton, 2011).

This study aims at exploring and understanding the weight/fingerprint of the multidecadal internal variability in the estimation of GHG-forced precipitation changes in the tropics using the Centre National de Recherches

Meteorologiques Coupled global climate Model, version 5 (CNRM-CM5). Abrupt doubling CO₂ experiments have been carried out to extract the forced response. Multimember ensembles are built here to evaluate the sensitivity (or interaction) of the forced response to (with) the variability of the Atlantic Meridional Overturning Circulation (AMOC). In CNRM-CM5, AMOC fluctuations are associated with surface ocean fingerprint, which projects on the so-called Atlantic Multidecadal Variability (AMV) pattern. In this model, the AMV corresponds to the leading mode of surface temperature internal low-frequency variability at global scale. Spectral analysis shows maximum energy concentration within the 80- to 120-year band as assessed from the long 850-year preindustrial control (piControl) experiment (Ruprich-Robert & Cassou, 2015) produced for the fifth phase of the Coupled Model Intercomparison Project (CMIP5; Taylor et al., 2012).

In the following, abrupt CO₂-doubling experiments are initialized from two extreme phases of the model AMOC and the impact of the initial ocean state on the tropical precipitation forced response is analyzed by contrasting the two distinct ensembles. Each of them includes 10 members differing by their first day atmospheric states so that the full range of uncertainties associated with internal variability (ocean + atmosphere) is covered—because of the combination of both macro and micro perturbations for the ensemble generation, following Hawkins et al. (2016) terminology. This protocol contrasts to most previous studies, which either combine single model realization from several models (Long et al., 2016; Oueslati et al., 2016; Vecchi & Soden, 2007) or which assess uncertainties through the sole atmospheric state sensitivity (Deser et al., 2012; Kang et al., 2013; Selten et al., 2004).

The rationale for the choice of selecting two contrasted states of AMOC internal variability from a given model relies on the fact that observational records over the historical period (on which anthropogenic forcing is active) are too short to know the actual stage of AMOC with respect to its own long-term variability. This is an irreducible source of uncertainties for the forced response, which should be quantified and better understood.

The rest of the paper is outlined as follows. The model simulations and methodology are described in section 2. Following an overview of the AMOC fingerprints in the CNRM-CM5 Model (section 3), we analyze the sensitivity of the projected changes in tropical precipitation and circulation to the strength of the AMOC (section 4) and propose a physical interpretation (section 5). Conclusions and discussion are given in section 6.

2. Materials and Method

2.1. Climate Model Simulations

We use the CNRM-CM5.1 Coupled General Circulation Model developed for CMIP5. The atmospheric component is the spectral ARPEGE-Climat-5.2 model, with a Gaussian grid of $\sim 1.4^\circ$ horizontal resolution and a vertical discretization over 31 levels (including 26 levels in the troposphere). The ocean model is Nucleus for European Modeling of the Ocean on the grid of $\sim 1^\circ$ horizontal resolution and a vertical discretization over 42 levels (including 18 levels in the upper 250-m mixed layer ocean). See Voltaire et al. (2013) for a complete description of the model.

Oceanic conditions of 1 January of year 303 and 141 are selected from the 850-year piControl experiment of CNRM-CM5 for the production of two unforced ensembles of 30 years and 10 members each. These two dates correspond to extreme opposite states of the AMOC in piControl (-4.1 and $+2.8$ standard deviation, respectively) associated with very pronounced negative and positive phases of AMV, respectively (see Figure 4 in Ruprich-Robert & Cassou, 2015). Individual members of each ensemble (hereafter referred to as Pcold and Pwarm) differ only by their atmospheric initial conditions, chosen randomly (see Ménégot et al., 2017, for a complete description of the protocol). Two twin ensemble experiments (i.e., identical initial conditions) are conducted (hereafter referred to as Fcold and Fwarm) with an instantaneous doubling of atmospheric CO₂ (abrupt2xCO₂ relative to preindustrial conditions using CMIP5 nomenclature) imposed at the beginning of the simulations and then hold fixed.

2.2. Calculations and Notations

Here are the calculations and notations of the different metrics applied on annually averaged fields from the ensembles.

- ΔX is the projected climate response to CO₂ abrupt doubling for a given ensemble ($X_f - X_p$). When applicable, we evaluate both the 30-year averaged change and the contribution arising from the first year only (as an approximation of the direct CO₂-forced fast response; Bony et al., 2013).
- δX stands for the anomaly of a given member with respect to the two-ensemble mean. ∂X is the anomaly expressed in percentage or fractional difference (relative to the two-ensemble mean).

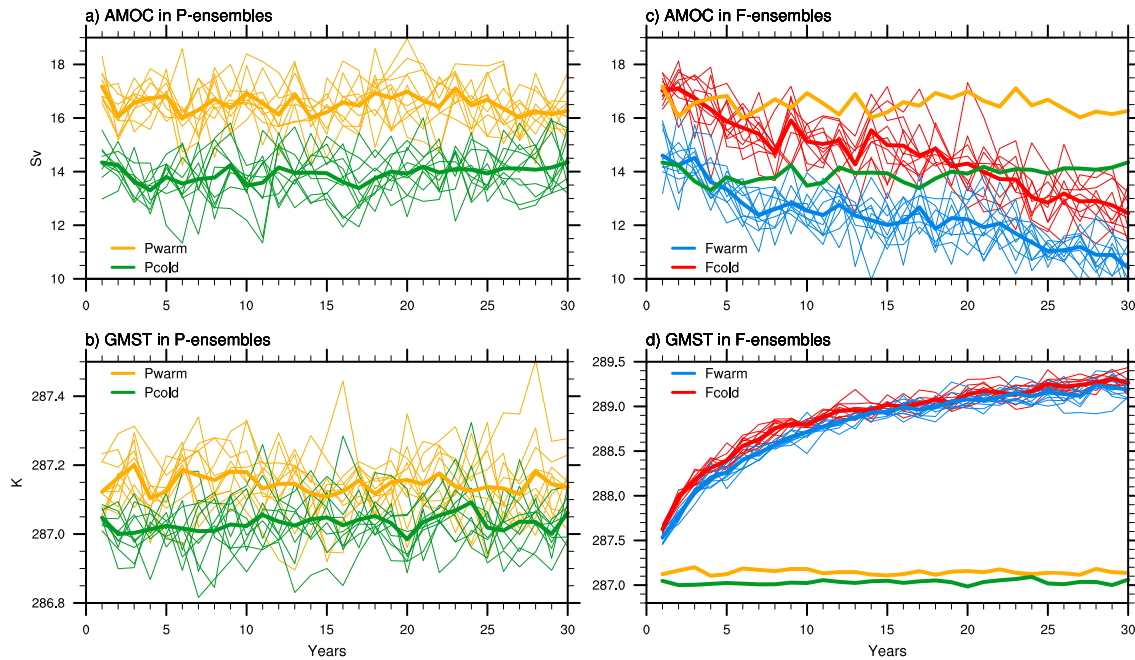


Figure 1. Yearly evolution of (a) AMOC and (b) GMST for Pwarm (orange) and Pcold (green) ensembles. Thin lines stand for individual members and thick lines for ensemble means. (c, d) Same as Figures 1a and 1b but for Fwarm (red) and Fcold (blue) ensembles, with the P ensemble mean quantities reproduced for reference. AMOC = Atlantic Multidecadal Overturning Circulation; GMST = global mean surface temperature.

- The statistical significance of AMOC-related ensemble mean differences (based upon $p < 0.10$, unless otherwise stated) is evaluated against a null hypothesis of zero change using a two-sided Student's t test.
- I refers to as the tropical atmospheric overturning circulation index defined by Bony et al. (2013). $I \equiv \omega_{500} \downarrow - \omega_{500} \uparrow$ with upward ($\omega_{500} \uparrow < 0$) and downward ($\omega_{500} \downarrow > 0$) pressure vertical velocities at 500 hPa averaged over $35^\circ\text{S} - 35^\circ\text{N}$.
- H is the Hadley circulation index defined as I but on zonally averaged values of ω_{500} over $35^\circ\text{S} - 35^\circ\text{N}$.
- W is the Pacific Walker circulation index defined as the difference between $\omega_{500} \uparrow$ over the western/central Pacific ($15^\circ\text{S} - 15^\circ\text{N}$, $110^\circ\text{E} - 160^\circ\text{W}$) and $\omega_{500} \downarrow$ over the eastern basin ($15^\circ\text{S} - 15^\circ\text{N}$, $80^\circ - 140^\circ\text{W}$). When applicable, we compute W over land + ocean or just ocean areas.
- The top of the atmosphere (TOA) instantaneous radiative forcing (IRF) quantifies the direct radiative impact of the doubling CO_2 concentration alone. It is commonly diagnosed from offline radiative transfer simulations (e.g., Collins et al., 2006), but due to the large number of ensemble experiments considered, we use the simple linear (least squares) regression model developed by Huang et al. (2016): $\text{IRF} = \overline{\text{IRF}} + \sum_i A_i \frac{y_i - \bar{y}_i}{\bar{y}_i}$, where A_i is the regression coefficient of a dependent variable y_i , with global mean multiyear mean \bar{y}_i , and $\overline{\text{IRF}}$, the intercept of the regression model, represents the global mean of IRF. This regression model accounts for several dependent variables i , which are taken from the P ensemble simulations, including the temperature at the surface and at 10 hPa, the vertically integrated water vapor, and the cloud radiative forcing (difference between all-sky and clear-sky radiation fluxes at the TOA). See Huang et al. (2016) for more details.
- R_a refers to the column-integrated atmospheric radiative fluxes ($R_a = R_{\text{TOA}} - R_{\text{SFC}}$, positive fluxes upward). The first-year change in R_a is used as an approximation of the direct CO_2 -forced radiative heating in the atmosphere.
- $\delta_x \text{IRF}$ and $\delta_x R_a$ are zonal gradients of IRF and R_a over the equatorial Pacific estimated by the difference between ($15^\circ\text{S} - 15^\circ\text{N}$, $110^\circ\text{E} - 160^\circ\text{W}$) and ($15^\circ\text{S} - 15^\circ\text{N}$, $80^\circ - 140^\circ\text{W}$), as in W calculation.

3. AMOC Fingerprints in CNRM-CM5

Figure 1 illustrates the yearly evolution of AMOC and global mean surface temperature (GMST) for the two 10-member P and F ensembles over the 30 years of integration. The model exhibits significant and persistent initial value predictability for both quantities as expected from spectral properties and physical mechanisms of AMOC variability assessed from piControl (Ruprich-Robert & Cassou, 2015). The 10-member Pcold and

Pwarm ensembles for the AMOC time series are clearly disjoint throughout the entire 30 years of simulations (Figure 1a). This is a fortiori true for AMOC ensemble means, as well as for GMST, with a difference of ~ 2.5 Sv and 0.11 °C, respectively.

Regionally, the AMOC fingerprints in CNRM-CM5 are consistent with previous inferences from observations and model-based studies (see Buckley & Marshall, 2016, for a review). Difference between Pcold and Pwarm ensembles show a significant (marginal) surface and tropospheric cooling (warming) over the Northern (Southern) Hemisphere when AMOC is weak due to reduced northward ocean heat transport. A southward displacement of the Hadley circulation and Intertropical Convergence Zone-related precipitation from their climatological position is obtained consistently with the modification of the mean interhemispheric gradient (supporting information Figure S1 and Ménégoz et al., 2017, for further description). A contraction and reinforcement of the Walker cell branches in the Pacific is also noticeable. Therefore, the AMOC-related anomalies are planetary and persistent so that the two ensembles can be treated as samples for two contrasted mean background states set by pure internal variability.

AMOC declines steadily in response to abrupt CO₂ forcing, but the two ensembles clearly remain disjoint over the 30-year integration (Figure 1c). Rapid warming occurs in both *F* ensembles, which stay statistically distinguishable in GMST up to ~ 15 years (Figure 1d). These emphasize on the very strong persistence properties of AMOC in the model despite extreme forcing perturbation.

4. Sensitivity of Precipitation and Circulation Forced Responses to AMOC States

The tropical precipitation and tropospheric circulation responses to CO₂ forcing and their modulation by different AMOC-related background states are presented in Figure 2. The CNRM-CM5 model exhibits increased rainfall in most of the deep tropics and enhanced drying over subtropical regions, similar to previous CMIP3/CMIP5 assessments (e.g., Long et al., 2016; Oueslati et al., 2016; Seager et al., 2010; Xie et al., 2015). Focus is laid on the tropical Pacific region, as it is where the fingerprint of multidecadal internal variability in the forced responses is the most important. Differences in rainfall changes between the cold and warm AMOC-related states are in the same order of magnitude (Figure 2c) as the individual CO₂-induced response assessed from ensemble mean changes (Figures 2a and 2b). This clearly indicates that AMOC is an important modulator of the projected forced changes in this region. Comparison of Figures 2c and 2f shows that the impact of different AMOC states on precipitation forced responses is strongly related to circulation changes (pattern correlation is equal to 0.95). A stepwise analysis of the vertically integrated water budget equation further demonstrates that the mean circulation changes alone can provide a full accounting of the difference in the equatorial Pacific rainfall changes between the cold and warm ensembles (supporting information Figures S2 to S4). Moreover, a decomposition of Figure 2f into its zonally averaged and zonally asymmetric component suggests that most of the modulation in rainfall changes originates from differences in the Walker circulation changes rather than in the Hadley circulation changes (supporting information Figure S5). The overall weakening of the Walker circulation (defined in section 2.2) is amplified by a factor of 2 in the cold ensemble (Figure 2g). This occurs almost everywhere across equatorial Pacific but more particularly over the ocean (Figures 2d–2f). We further show that the direct CO₂-forced Walker circulation response (Figure 2h), rather than the temperature-mediated transient circulation response (Figure 2i), explains to a large extent the sensitivity of precipitation forced changes to AMOC states. Figure 2h shows a significant initial value predictability of the direct CO₂-forced Walker circulation responses. The large range of projected changes in Walker circulation depends on its climatological strength: the Walker circulation is more strongly reduced when it is stronger a priori in the preindustrial control climate state (Figure 2h). This relationship is even stronger when *W* is computed over ocean areas only (correlation $R = 0.7$ —not shown).

In the next section, we investigate the physical mechanism controlling these contrasted circulation responses to CO₂ forcing. To this end, we address two questions: (i) How do different AMOC-related states influence the tropical mean circulation in the control climate state? (section 5.1); (ii) Why does the direct circulation response to increased CO₂ depend on the mean background state? (section 5.2).

5. Physical Understanding

5.1. AMOC-Related Influence on Tropical Circulation in Control Climate

Global constraints on precipitation and water vapor are commonly used to understand the tropical circulation response to global warming (e.g., Held & Soden, 2006; Mitchell et al., 1987; Vecchi & Soden, 2007). We here

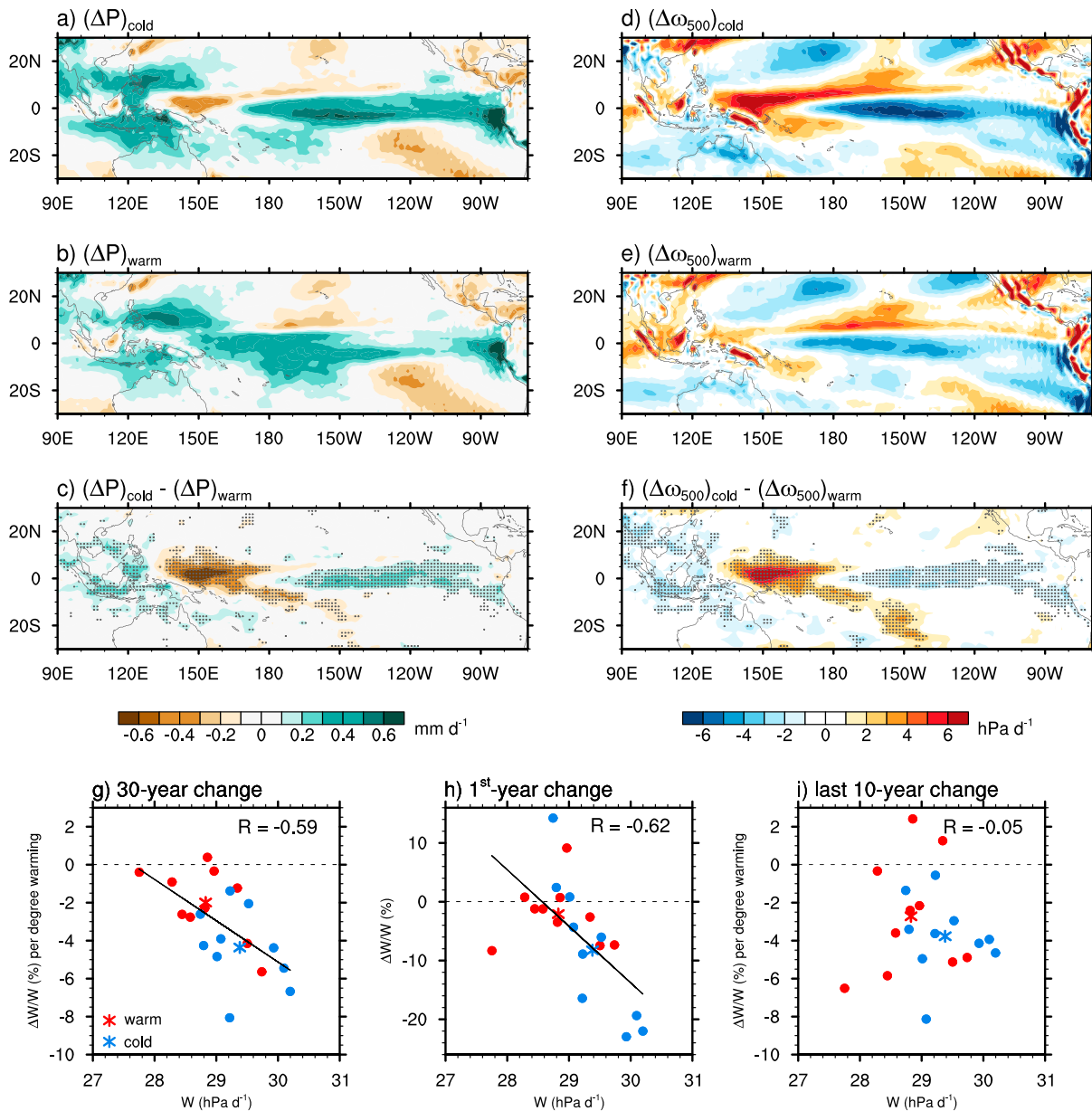


Figure 2. (a–c) The 30-year mean response to CO₂ forcing in precipitation for (a) cold and (b) warm ensemble means over tropical Pacific (30°S–30°N, 90°E–70°W) and (c) AMOC-related difference between cold and warm ensembles (hatching indicating statistical significance). (d–f) Same as Figures 2a–2c but for pressure vertical velocity at 500 hPa. (g–i) Fractional forced changes (relative to *P* ensembles) in Walker circulation as a function of its mean intensity in *P* ensembles for warm (red) and cold (blue) ensembles: (g) 30-year mean change per degree of global surface warming, (h) first-year change and (i) last 10-year mean change per degree of global surface warming. Each individual member is represented by a filled circle and the ensemble means by asterisks.

apply the same energetic constraints to explain the sensitivity of the tropical mean overturning circulation to the AMOC state, since the latter has a global influence on the modeled climate (Figure 1b and supporting information Figure S1) and thus justifies the use of such a conceptual framework.

When the AMOC is weaker in control experiments, the surface temperature decreases significantly by 0.11 K (globally) and by 0.04 K (in the tropics). As shown in Figure 3, this decrease in temperature is also associated with (i) a decrease in precipitation of 1.6%/K (Figure 3a) that results from a weaker radiative cooling and surface evaporation (not shown) and (ii) a decrease in column water vapor amount following the Clausius-Clapeyron constraint of 7%/K (Figure 3b). Following Mitchell et al. (1987), this differential response of the tropical (or equivalently global) mean decrease in precipitation and humidity to surface cooling can be used to estimate the fractional increase of the tropical overturning circulation in response to surface cooling. Using $\delta M/M =$

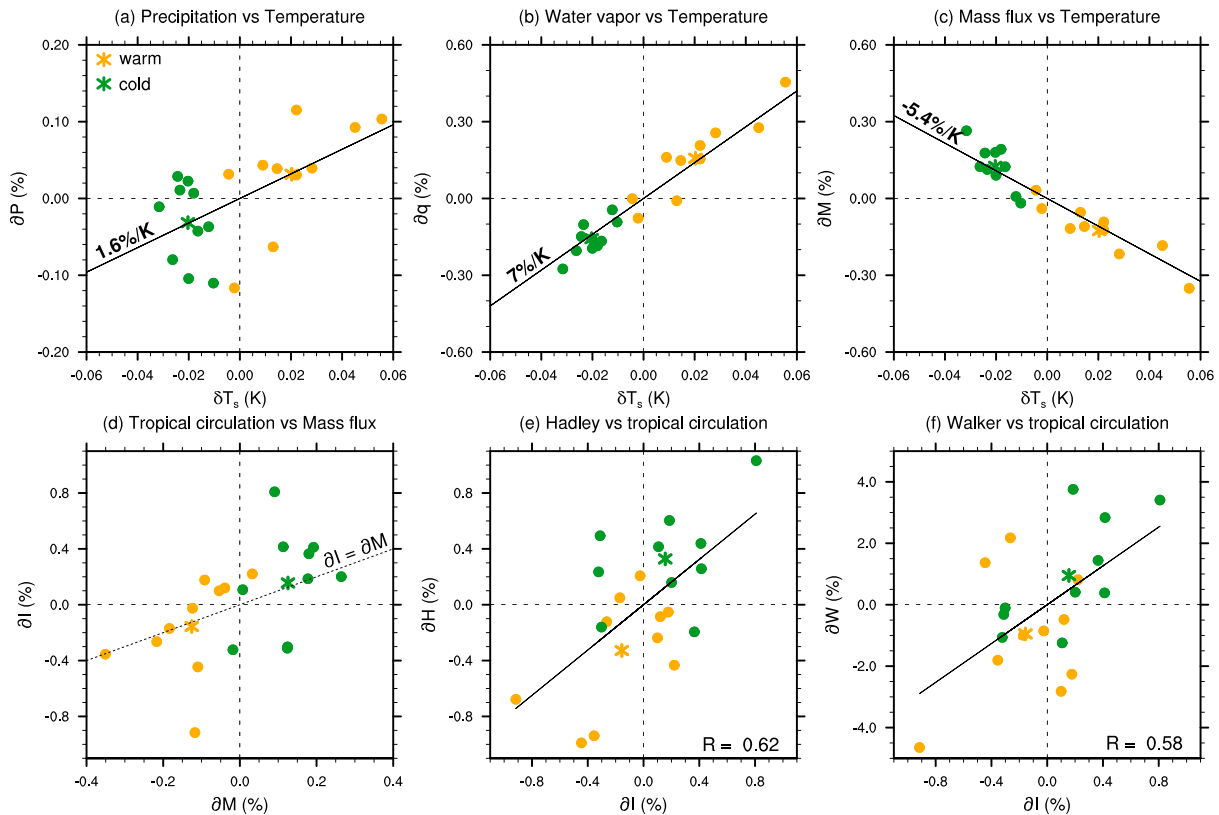


Figure 3. AMOC-related fractional differences (∂X in section 2.2) for tropically averaged (a) precipitation, (b) vertically integrated water vapor, and (c) convective mass flux—estimated as the difference between Figures 3a and 3b as in Vecchi and Soden (2007)—as a function of AMOC-related absolute differences in tropically averaged surface temperature (δT_s , in Kelvin). (d–f) AMOC-related fractional differences for the tropically averaged (d) overturning circulation, (e) Hadley circulation, and (f) Walker circulation as a function of AMOC-related fractional differences in the estimated tropical convective mass flux (in Figure 3d) and in the simulated overturning circulation (in Figures 3e and 3f). All differences are significant at $p < 0.03$. The color code is the same as Figure 1 for P ensembles; warm (orange) and cold (green) members are shown by filled circles and their respective ensemble means by asterisks. Also reported in Figures 3a–3c is the slope of the least squares regression fits (solid lines). In Figure 3d the dashed line highlights the one-to-one relationship between ∂I and ∂M . AMOC = Atlantic Multidecadal Overturning Circulation.

$\delta P/P - 0.07\delta T_s/T_s$ (Held & Soden, 2006; Vecchi & Soden, 2007), where M is the convective mass flux, P is the precipitation, and T_s the surface temperature, we expect an overall strengthening of the convective mass fluxes by 5.4%/K in the cold ensemble (Figure 3c). The relationship between this theoretical strengthening in convective mass flux and the actual change in the overturning circulation simulated by the model is fairly good with ensemble means lying right on top of the expected line set by the theory (Figure 3d). This confirms that the influence of AMOC on the tropical mean circulation corresponding to pure by-products of internal climate processes can be very well explained by the latter conceptual framework.

The AMOC-related change in the tropical overturning circulation is also reflected in the Hadley and Walker circulations, which are significantly reinforced when AMOC is weaker (Figures 3e and 3f). Note that other factors control the Hadley and Walker circulations, influencing the exact magnitude of their AMOC-forced intensification and their relationships to the tropical mean overturning circulation. These factors could result from a redistribution of the convective and subsiding areas, which often accompanies the change in the intensity of the tropical overturning circulation (e.g., Vecchi & Soden, 2007) or in the northward ocean heat transport (e.g., L'hévéder et al., 2015). When AMOC is weak, the overall strengthening of the Walker and Hadley circulations is here associated with an eastward shift of convection over the central equatorial Pacific (supporting information Figure S1d) and a southward shift of the Hadley circulation, resulting in a strengthening (weakening) of the northern (southern) cell (supporting information Figure S1e). Despite this phenomenon, our analysis suggests that the global constraints on precipitation and water vapor are useful to understand not only the mean circulation weakening with global surface warming but also the relationship between the multidecadal variations of the GMST and of the tropical overturning circulation (Hadley/Walker) associated

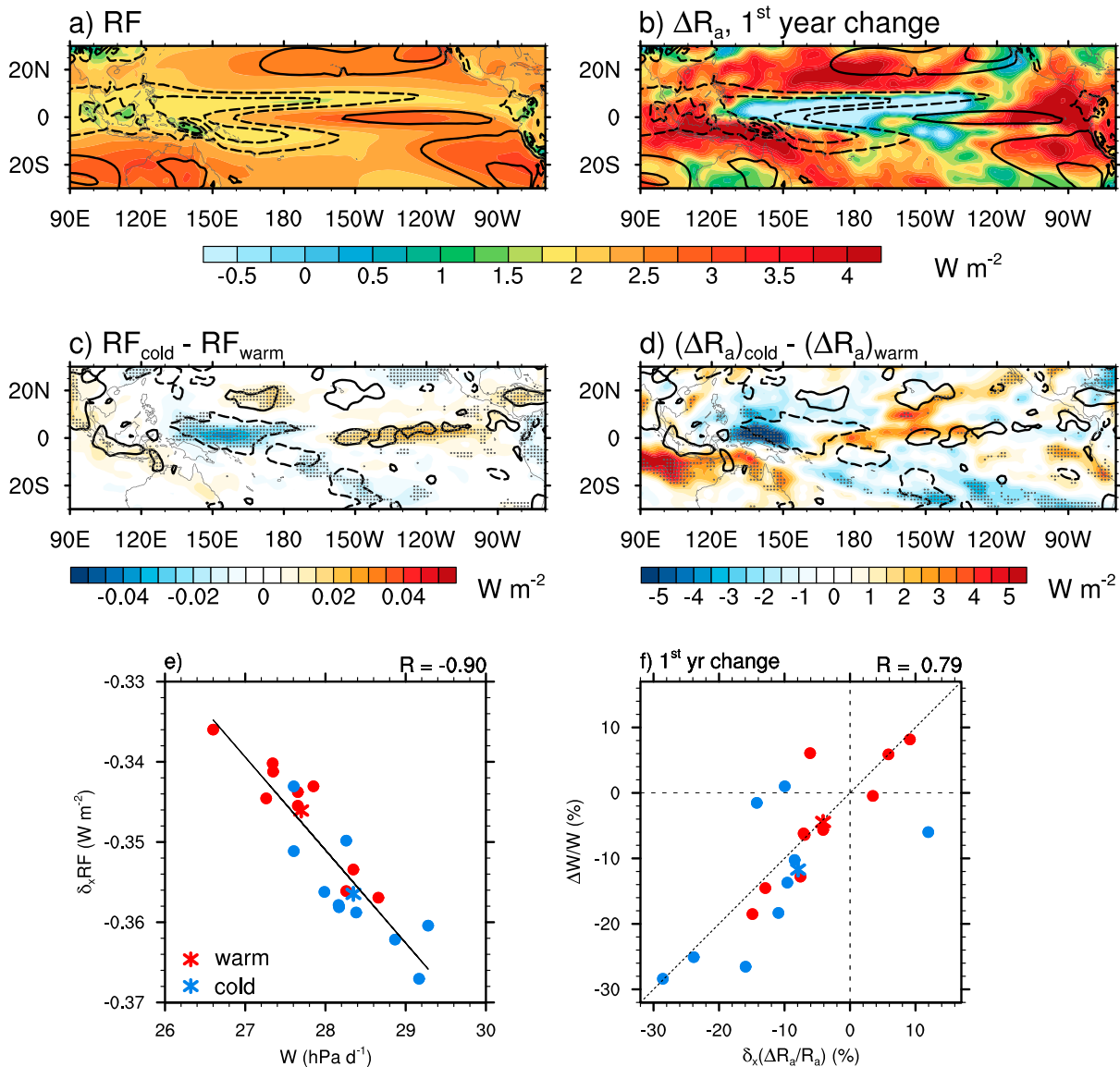


Figure 4. (a, b) The two-ensemble mean (a) IRF and (b) first-year ΔR_a (shaded) and 30-year mean ω_{500} for the P ensembles (overlaid). (c, d) AMOC-related difference for (c) IRF and (d) ΔR_a ; hatching indicates statistical significance, and overlaid contours show the AMOC-related difference in ω_{500} . (e) Zonal gradient in IRF ($\partial_x IRF$) as a function of Walker circulation in the P ensembles. (f) First-year fractional change (compared with P ensembles) in Walker circulation as a function of first-year fractional change in $\partial_x \Delta R_a$. W is computed over ocean areas only to ensure that the relationships are not influenced by land-sea contrasts. The legend is similar to Figure 2: warm (red) and cold (blue) members are shown by filled circles and their respective ensemble means by asterisks. IRF = instantaneous radiative forcing; AMOC = Atlantic Multidecadal Overturning Circulation.

with the AMOC internally generated fluctuations. These results are robust across a large ensemble of CMIP5 models, except maybe for the AMOC-related variations in the Hadley circulation, which appear more model dependent (supporting information Text S2 and Figure S6).

5.2. Dependence of the Direct CO_2 -Forced Response on the Background State

We now explore the reasons why the direct effect of CO_2 on the Walker circulation depends on the climatological strength of the Walker circulation in the preindustrial climate state and thus on the state of the AMOC (Figure 2h). One mechanism, proposed by Merlis (2015), relates the direct weakening of the overturning circulation to the spatial structure of the IRF to increased CO_2 . The argument is based on the moist energetics of the tropical atmosphere, which constrain the mean overturning circulation to export energy from energy-rich (warm/moist) regions toward relatively energy poor (cold/dry) regions (Neelin & Held, 1987; Trenberth & Stepaniak, 2004).

As shown by Huang et al. (2016), the spatial structure of the IRF strongly depends on the horizontal gradients of atmospheric and surface variables of the control climate state, especially surface and atmospheric temperature, atmospheric humidity, and clouds. Figure 4a shows that the IRF (as estimated by Huang et al., 2016; see also section 2.2) is stronger (weaker) in regions of large-scale subsiding (rising) motions (compare IRF with black contours in Figure 4a). This dependence of the forcing on the mean circulation is explained by the presence of deep convective clouds and strong water vapor mixing ratios in regions of large-scale ascent, which masks the effect of increased CO₂ on TOA radiative fluxes (Huang et al., 2016, 2017; Merlis, 2015; Xia & Huang, 2017). Over the tropical oceans, much of the IRF is confined to the atmosphere (e.g., Huang et al., 2017; Xia & Huang, 2017). Therefore, the effect of the spatially inhomogeneous IRF, shown in Figure 4a, is to radiatively heat the atmosphere more strongly in the subsiding than ascending region (as suggested in Figure 4b by the first-year change in R_a), which then requires the circulation to weaken to restore local atmospheric energetics. It is also worth noting that in the tropics, clouds and humidity interact with the circulation in a positive feedback loop, such that even small spatial gradients in IRF could lead to a substantial circulation weakening within the first year. This would occur if the initial weakening of the circulation acts to reinforce the spatial pattern of the IRF, for instance, by reducing (enhancing) moisture and convective cloud development—and thus atmospheric radiative heating—over the climatological ascending (subsiding) region. Such forcing adjustment mechanism (following the terminology from forcing-feedback studies; e.g., Chung & Soden, 2015; Sherwood et al., 2015) is here assumed based on the larger magnitude of the spatial gradients in the first-year ΔR_a than in the IRF (Figures 4a and 4b) and the presumably small contribution from surface to the IRF at TOA (Chung & Soden, 2015; Huang et al., 2017; Xia & Huang, 2017).

Overall, these considerations suggest that when the tropical overturning circulation is stronger in the control climate state, cloud and water vapor gradients between convective and subsidence areas are reinforced, and the larger spatial heterogeneity of the CO₂ forcing (IRF + adjustments) potentially leads to a stronger weakening of the circulation. Consistent with this interpretation and because the Walker circulation is stronger when the AMOC is weaker (in the cold ensemble), the TOA radiative forcing and first-year atmospheric radiative heating are found to be (i) stronger in the eastern equatorial Pacific, where the subsiding branch of circulation is stronger, and (ii) weaker in the central equatorial Pacific region, where the rising branch of circulation is stronger (Figures 4c–4e). Therefore, the stronger Pacific equatorial zonal gradient in radiative forcing that is produced in the cold ensemble is expected to induce a stronger weakening of the Walker circulation by the direct effect of CO₂ on the atmospheric radiative fluxes and subsequent rapid adjustments amplifying the walker circulation response (as suggested in Figure 4f).

6. Conclusion

In this study, the tropical precipitation and tropospheric circulation responses to CO₂ forcing and its modulation by different states of the AMOC have been investigated using multimember ensembles from the fully coupled CNRM-CM5 General Circulation Model. A very large range of possible precipitation projections is obtained in the equatorial Pacific region due to pure internal variability, assessed here through an ensemblist approach and a combination of macro and micro perturbations for its generation. The associated uncertainties are comparable to—or even larger than—the forced response estimated through ensemble mean changes. This underscores the crucial need for realizing multimember ensembles (by sampling both atmospheric and oceanic initial conditions) to better characterize the forced model's climate change projections, even for extreme forcing perturbations as is the case here.

Contrasted precipitation and circulation forced responses arise depending on the strength of the AMOC in the preindustrial climate state, used as initial states. When the AMOC is weaker, the slowdown of the Walker circulation in response to increased CO₂ is amplified (compared to when the AMOC is stronger), which substantially influences the amplitude of rainfall changes over Indonesia, Southeast Asia, and the equatorial Pacific Ocean. The direct CO₂-forced effect alone on circulation changes explains the overall sensitivity of precipitation and circulation forced changes to AMOC states. A mechanism is proposed to explain how the direct weakening of the tropical circulation in response to CO₂ depends on AMOC-related background climate states. We show the following.

1. Global energetic constraints on precipitation and water vapor explain the impact of different AMOC states on the mean tropical circulation in the control climate. When the AMOC is weak, a strengthening of the tropical overturning circulation (Hadley and Walker circulations) is obtained consistently with a significant decrease in GMST.

2. The direct weakening of the circulation in response to increased CO₂ results from the dependence of the CO₂ radiative forcing on the spatial distribution of clouds and water vapor (Merlis, 2015). Therefore, the stronger overturning circulation (when AMOC is weaker), which enhances the cloud and water vapor contrasts between convective and subsidence areas and thus the spatial heterogeneity of the CO₂ forcing, leads to a stronger direct weakening of the circulation.

Our interpretation provides an example of a new mechanism by which the response of tropical precipitation to CO₂ forcing depends on the background climate state. We call it the *strong-gets-weaker* mechanism, as it essentially operates through the circulation changes: the stronger the circulation in the control climate state, the weaker it gets in response to CO₂ forcing, enhancing the amplitude of rainfall changes at the regional scales. Although the example given here explains the AMOC influence on Walker circulation forced changes, this mechanism might also provide the backdrop for any factor that influences the intensity of the mean tropical circulation in the control climate state. A point that should motivate further investigation for understanding the intermodel spread in CO₂-forced circulation changes.

These insights are based on the analysis of abrupt doubling CO₂ experiments; the question arises as to how relevant they are to interpret the AMOC influence on the climate response to gradually increasing CO₂ concentration. We analyzed twin ensemble transient climate change simulations using the exact same initial conditions, in which CO₂ increases at 2% per year until doubling the initial CO₂ concentration. We found very similar ensemble mean sensitivities of precipitation and circulation forced changes to AMOC states (supporting information Figures S7–S14). Moreover, strong differences between respective members (from abrupt and transient CO₂ forcing experiments) are noticeable, despite the fact that they have the exact same initial conditions. This confirms the robustness of our results, which emphasize the very important role of the background climate state for the projected tropical and circulation changes, at least in the CNRM-CM5 model.

Acknowledgments

This work is supported by the French National Research Agency (ANR) project MORDICUS (ANR-13-SENV-0002-01). Primary data and scripts used in the analysis and other supporting information are archived at ftp://ftp.cerfacs.fr/pub/globc/exchanges/cassou/Data4Papers/GRL_Via_etal_2018/. We acknowledge the World Climate Research Programme's Working Group on Coupled Modelling, which is responsible for CMIP, and we thank the climate modeling groups (listed in Table S1 of this paper) for producing and making available their model output on the CEDA portal (<http://browse.ceda.ac.uk>). Additionally, we are grateful to the two reviewers for their helpful comments.

References

- Bony, S., Bellon, G., Klocke, D., Sherwood, S., Fermepin, S., & Denvil, S. (2013). Robust direct effect of carbon dioxide on tropical circulation and regional precipitation. *Nature Geoscience*, 6(6), 447–451.
- Buckley, M. W., & Marshall, J. (2016). Observations, inferences, and mechanisms of the Atlantic Meridional Overturning Circulation: A review. *Reviews of Geophysics*, 54, 5–63. <https://doi.org/10.1002/2015RG000493>
- Cassou, C., Kushnir, Y., Hawkins, E., Pirani, A., Kucharski, F., Kang, S., & Caltabiano, N. (2018). Decadal climate variability and predictability: Challenges and opportunities. *Bulletin of the American Meteorological Society*, 99(3), 479–490.
- Chadwick, R., Boutle, I., & Martin, G. (2013). Spatial patterns of precipitation change in CMIP5: Why the rich do not get richer in the tropics. *Journal of Climate*, 26(11), 3803–3822.
- Chou, C., & Neelin, J. D. (2004). Mechanisms of global warming impacts on regional tropical precipitation. *Journal of Climate*, 17(13), 2688–2701.
- Chou, C., Neelin, J. D., Chen, C.-A., & Tu, J.-Y. (2009). Evaluating the “rich-get-richer” mechanism in tropical precipitation change under global warming. *Journal of Climate*, 22(8), 1982–2005.
- Chung, E.-S., & Soden, B. J. (2015). An assessment of methods for computing radiative forcing in climate models. *Environmental Research Letters*, 10(7), 74004.
- Collins, W., Ramaswamy, V., Schwarzkopf, M., Sun, Y., Portmann, R., Fu, Q., et al. (2006). Radiative forcing by well-mixed greenhouse gases: Estimates from climate models in the intergovernmental panel on climate change (IPCC) fourth assessment report (ar4). *Journal of Geophysical Research*, 111, D14317. <https://doi.org/10.1029/2005JD006713>
- De Carvalho, L. M. V. (2016). *The monsoons and climate change: Observations and modeling*.
- Deser, C., Phillips, A., Bourdette, V., & Teng, H. (2012). Uncertainty in climate change projections: The role of internal variability. *Climate Dynamics*, 38(3–4), 527–546.
- Hawkins, E., Smith, R. S., Gregory, J. M., & Stainforth, D. A. (2016). Irreducible uncertainty in near-term climate projections. *Climate Dynamics*, 46(11–12), 3807–3819.
- Hawkins, E., & Sutton, R. (2011). The potential to narrow uncertainty in projections of regional precipitation change. *Climate Dynamics*, 37(1–2), 407–418.
- Held, I. M., & Soden, B. J. (2006). Robust responses of the hydrological cycle to global warming. *Journal of Climate*, 19(21), 5686–5699.
- Huang, Y., Tan, X., & Xia, Y. (2016). Inhomogeneous radiative forcing of homogeneous greenhouse gases. *Journal of Geophysical Research: Atmospheres*, 121, 2780–2789. <https://doi.org/10.1002/2015JD024569>
- Huang, Y., Xia, Y., & Tan, X. (2017). On the pattern of CO₂ radiative forcing and poleward energy transport. *Journal of Geophysical Research: Atmospheres*, 122, 10,578–10,593. <https://doi.org/10.1002/2017JD027221>
- Kang, S., Deser, C., & Polvani, L. M. (2013). Uncertainty in climate change projections of the Hadley circulation. *Journal of Climate*, 26, 7541–7554.
- L'hévéder, B., Codron, F., & Ghil, M. (2015). Impact of anomalous northward oceanic heat transport on global climate in a slab ocean setting. *Journal of Climate*, 28(7), 2650–2664.
- Long, S.-M., Xie, S.-P., & Liu, W. (2016). Uncertainty in tropical rainfall projections: Atmospheric circulation effect and the ocean coupling. *Journal of Climate*, 29(7), 2671–2687.
- Ma, J., & Xie, S.-P. (2013). Regional patterns of sea surface temperature change: A source of uncertainty in future projections of precipitation and atmospheric circulation. *Journal of Climate*, 26(8), 2482–2501.
- Ménégoz, M., Cassou, C., Swingedouw, D., Ruprich-Robert, Y., Bretonnière, P.-A., & Doblus-Reyes, F. (2017). Role of the Atlantic multidecadal variability in modulating the climate response to a Pinatubo-like volcanic eruption. *Climate Dynamics*. <https://doi.org/10.1007/s00382-017-3986-1>

- Merlis, T. M. (2015). Direct weakening of tropical circulations from masked CO₂ radiative forcing. *Proceedings of the National Academy of Sciences*, *112*(43), 13,167–13,171.
- Mitchell, J. F., Wilson, C., & Cunningham, W. (1987). On CO₂ climate sensitivity and model dependence of results. *Quarterly Journal of the Royal Meteorological Society*, *113*(475), 293–322.
- Neelin, J. D., & Held, I. M. (1987). Modeling tropical convergence based on the moist static energy budget. *Monthly Weather Review*, *115*(1), 3–12.
- Oueslati, B., Bony, S., Risi, C., & Dufresne, J.-L. (2016). Interpreting the inter-model spread in regional precipitation projections in the tropics: Role of surface evaporation and cloud radiative effects. *Climate dynamics*, *47*(9-10), 2801–2815.
- Ruprich-Robert, Y., & Cassou, C. (2015). Combined influences of seasonal east atlantic pattern and north atlantic oscillation to excite Atlantic multidecadal variability in a climate model. *Climate Dynamics*, *44*(1-2), 229–253.
- Seager, R., Naik, N., & Vecchi, G. A. (2010). Thermodynamic and dynamic mechanisms for large-scale changes in the hydrological cycle in response to global warming. *Journal of Climate*, *23*(17), 4651–4668.
- Selten, F. M., Branstator, G. W., Dijkstra, H. A., & Kliphuis, M. (2004). Tropical origins for recent and future Northern Hemisphere climate change. *Geophysical Research Letters*, *31*, L21205. <https://doi.org/10.1029/2004GL020739>
- Sherwood, S. C., Bony, S., Boucher, O., Bretherton, C., Forster, P. M., Gregory, J. M., & Stevens, B. (2015). Adjustments in the forcing-feedback framework for understanding climate change. *Bulletin of the American Meteorological Society*, *96*(2), 217–228.
- Taylor, K. E., Stouffer, R. J., & Meehl, G. A. (2012). An overview of CMIP5 and the experiment design. *Bulletin of the American Meteorological Society*, *93*(4), 485–498.
- Trenberth, K. E., & Stepaniak, D. P. (2004). The flow of energy through the Earth's climate system. *Quarterly Journal of the Royal Meteorological Society*, *130*(603), 2677–2701.
- Vecchi, G. A., & Soden, B. J. (2007). Global warming and the weakening of the tropical circulation. *Journal of Climate*, *20*(17), 4316–4340.
- Voltaire, A., Sanchez-Gomez, E., y Méliá, D. S., Decharme, B., Cassou, C., Sénézi, S., et al. (2013). The CNRM-CM5.1 global climate model: Description and basic evaluation. *Climate Dynamics*, *40*(9-10), 2091–2121.
- Xia, Y., & Huang, Y. (2017). Differential radiative heating drives tropical atmospheric circulation weakening. *Geophysical Research Letters*, *44*, 10,592–10,600. <https://doi.org/10.1002/2017GL075678>
- Xie, S.-P., Deser, C., Vecchi, G. A., Collins, M., Delworth, T. L., Hall, A., et al. (2015). Towards predictive understanding of regional climate change. *Nature Climate Change*, *5*(10), 921.
- Xie, S.-P., Deser, C., Vecchi, G. A., Ma, J., Teng, H., & Wittenberg, A. T. (2010). Global warming pattern formation: Sea surface temperature and rainfall. *Journal of Climate*, *23*(4), 966–986.